Nuclear structure of ^{94,95}Mo at high spins

B. Kharraja,* S. S. Ghugre,† and U. Garg
Department of Physics, University of Notre Dame, Notre Dame, Indiana 46556

R. V. F. Janssens, M. P. Carpenter, B. Crowell,‡ T. L. Khoo, T. Lauritsen, and D. Nisius
Physics Division, Argonne National Laboratory, Argonne, Illinois 60439

W. Reviol, W. F. Mueller, and L. L. Riedinger
Department of Physics, University of Tennessee, Knoxville, Tennessee 37996

R. Kaczarowski
Soltan Institute for Nuclear Studies, 05-400 Swierk, Poland
(Received 28 January 1998)

The high-spin level structures of ^{94,95}Mo ($N=52,53$) have been investigated via the ^{65}Cu(^{36}S, $\alpha p2n$)^{94}Mo and ^{65}Cu(^{36}S, αpn)^{95}Mo reactions at 142 MeV. The level schemes have been extended up to spin $J\approx 19\hbar$ and excitation energies $E_x\approx 12$ MeV. Spherical shell-model calculations have been performed and compared with the experimental energy levels. The level structure of ^{94}Mo exhibits a single-particle nature and the higher-angular-momentum states are dominated by the excitation of a $g_{9/2}$ neutron across the $N=50$ shell gap. The level sequences observed in ^{95}Mo have been interpreted on the basis of the spherical shell model and weak coupling of a $d_{5/2}$ or a $g_{7/2}$ neutron to the ^{94}Mo core.
[S0556-2813(98)02306-1]

PACS number(s): 27.60.+j, 23.20.Lv, 21.60.Cs

I. INTRODUCTION

This investigation of the high-spin states of ^{94,95}Mo is a continuation of efforts to understand the level structure of nuclei located just above the $N=50$ shell closure [1,2]. The low-spin levels of these nuclei have been previously studied [3–5] and interpreted within the framework of either the spherical shell model and/or vibrational models [6]. The low-lying levels of nuclei with $N=50$ are dominated by $\pi(p_{1/2},g_{9/2})$ proton excitations [7]. Numerous additional excitations [for example, neutron excitations within the $(d_{5/2},s_{1/2},g_{7/2},h_{11/2})$ orbitals coupled to the proton excitations within the $(p_{1/2},g_{9/2})$ orbitals] are also possible for the low-lying levels in nuclei with $N>50$. With the advent of heavy-ion accelerators and modern arrays of Compton-suppressed Ge detectors, it is now possible to extend the level schemes of these nuclei into the higher-angular-momentum regimes.

The level structure of nuclei with $N\leqslant 51$ exhibits single-particle behavior, even at high spins [1,2,8,9]. However, not much experimental information is available on the level structures of nuclei with $52\leqslant N\leqslant 54$ at comparable angular momenta. Investigations of the level structures in the high-angular-momentum domain would contribute to (i) the understanding of the mechanisms responsible for the generation of high-spin states and (ii) probing of the possible onset of collectivity in this mass region and the transition from single-particle to collective behavior.

A recent study of high-spin states in ^{92}Mo ($N=50$) [9] indicates that the level structure in this nucleus exhibits single-particle character even at spins as high as $J\approx 18\hbar$. Earlier studies of ^{94,95}Mo had employed α particles as the incident projectile [3–5]. The results presented in the present paper on the ^{94,95}Mo nuclei were obtained as a by-product of the study of $^{96-98}$Ru, reported in [10]. Although, the cross sections for the production of the ^{94,95}Mo isotopes were rather small (8.0% and 4.3% of the total fusion cross section, respectively), interesting information was extracted on these nuclei. This was due in part to the use of a ^{36}S projectile capable of imparting large amounts of angular momentum to the nuclei of interest and in part to the detection sensitivity of Gammasphere, a multidetector array of the newest generation.

II. EXPERIMENTAL PROCEDURE

High-spin states in ^{94,95}Mo were populated via the ^{65}Cu(^{36}S, αpxn) reactions ($x=2$ and 1, respectively), at a bombarding energy of 142 MeV. Even though the incident beam energy was not optimized (according to statistical model calculations) for the ^{94,95}Mo reaction channels, it was still possible to obtain substantial information on the higher-angular-momentum states in these nuclei, as can be seen below. The ^{36}S beam was provided by the 88-Inch Cyclotron facility at the Ernest O. Lawrence Berkeley National Laboratory. Two stacked, self-supporting, isotopically enriched ^{65}Cu target foils ($\sim$0.5 mg/cm^2 thick) were used. Triple- and higher-fold coincidence events were measured using the early implementation phase of the Gammasphere array,

*On leave from Physics Department, University Chouaib Doukkali, BP 20, El Jadida, Morocco.

†Present address: IUCDAEF-Calcutta Center, Sector III/LB-8, Bidhan Nagar, Calcutta 700 064, India.

‡Present address: Fullerton Community College, Fullerton, CA 92833.

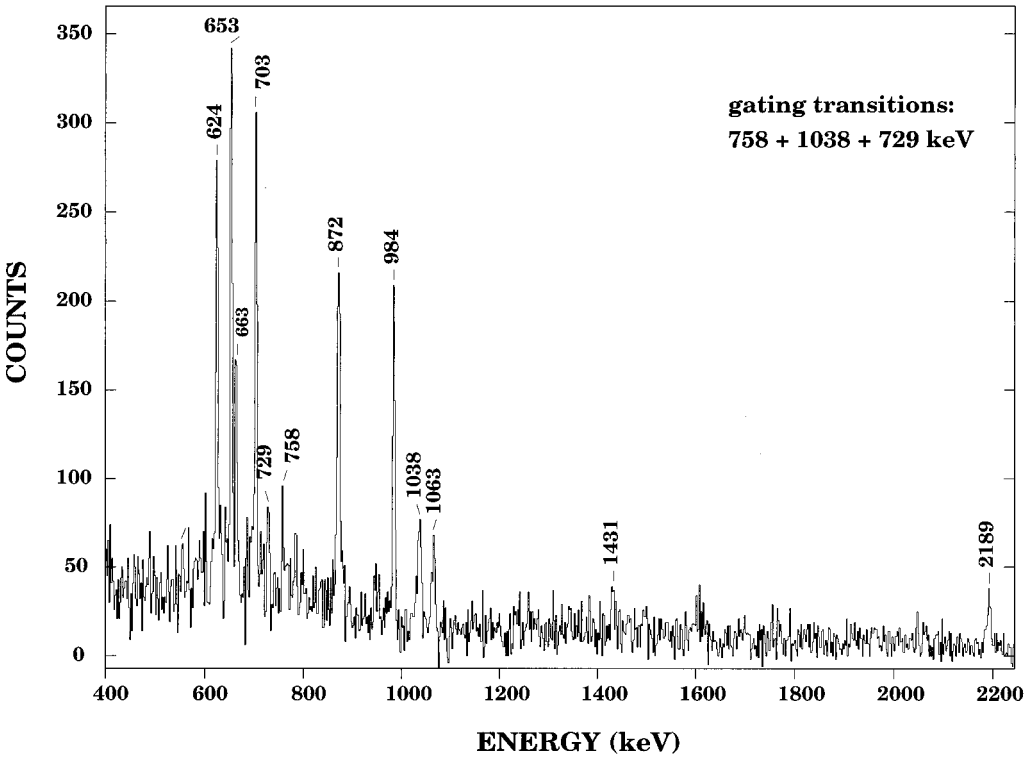

FIG. 1. Representative double-gated coincidence γ spectrum for ^{94}Mo. All transition energies are marked to within ± 1 keV.

which at that time comprised 36 Compton-suppressed Ge detectors. A total of about 400×10^6 events were accumulated and stored onto magnetic tapes for further analysis.

The data were sorted into three-dimensional histograms (E_γ-E_γ-E_γ cubes) using the Radware [11] and Kuehner [12] formats. The coincidence cube with Radware format was analyzed with the Radware software package [13] which uses the generalized background subtraction algorithm of Ref. [14] to extract spectra corresponding to two coincidence gates (the so-called ''double-gated spectra''). Such double-gated spectra were also obtained from the Kuehner cube using the FUL method of background subtraction [15]. More experimental details, including procedures for constructing level schemes and for multipolarity assignments, are given in Ref. [10]. In particular, multipolarity assignments were based primarily on intensity ratios extracted from angle-sorted matrices: coincidence gates were placed on transitions detected in the forward-angle (32° and 37°) detectors, and the γ rays measured at 90° and at backward angles (143° and 147°) were sorted along the two axes of the matrices. Although, as pointed out in Ref. [10], such directional correlation (DCD) ratios $R=I_\gamma$(backward)/I_γ(90°) have their limitations, reliable spin assignments can still be made by comparing the ratios of the new γ lines to those of previously known γ rays whose multipolarity is already firmly established [3,4]. In the present configuration, γ rays of $E2$ character have $R\approx1.9$, whereas dipole transitions have $R\approx1.5$.

III. RESULTS

Thirty-three new γ rays belonging to ^{94}Mo were observed in the present work. Figure 1 illustrates the quality of the data with a double-gated coincidence spectrum on transitions in ^{94}Mo. The measured spectroscopic data (γ-ray energies, intensities, DCO ratios, and suggested spin assignments) are summarized in Table I and the proposed ^{94}Mo level scheme is shown in Fig. 2. The new γ rays extending the previously known positive-parity cascade beyond the 10^+ state [3] are of energies 241, 443, 487, 715, 791, 974, 1060, 1245, 1341, 1367, 1609, 1612, 1740, 1750, 2096, and 2389 keV, respectively. The ordering of these transitions is based on the measured intensities and the observed coincidence patterns. All these transitions have been assigned an $M1$ multipolarity, based on a comparison of the obtained DCO ratio values with the previously known $M1$ γ rays, systematics of level structures in this region [2,10,16], and comparisons with shell-model calculations (see below). In particular, the DCO ratios of these transitions, where available, are larger than the values generally associated with pure $E1$ transitions, and are similar to those for $M1$ transitions with strong $E2$ admixtures (for more details, see Ref. [10]). This cascade is, thus, extended up to $J=(18^+)$ and $E_x\approx12$ MeV. It may be noted that no transitions deexciting the level fed by the 487-keV transition [$J^\pi=(13^+)$, $E_x\approx7$ MeV] have been observed, suggesting either that the intensity is fragmented into many weak transitions or that this level is an isomeric state (the use of a thin target precluded identification of possible isomers).

The new transitions belonging to the proposed negative-parity cascade and feeding the 7^- level [3] are also mostly of $M1$ character (except where indicated) and are of energies 555, 565, 624, 653($E2$), 663, 729($E2$),984($E2$), 1063, 1431, 1600, and 2189 keV, respectively. This structure has been extended up to $J=(17^-)$ and $E_x\approx10$ MeV. In addition, the 251-, 308-, 367-, 945-, and 1543-keV transitions were found to connect the positive- and negative-parity cascades,

TABLE I. Energies, initial and final spins, relative intensities, and ratios R (as defined in the text) for transitions assigned to ^{94}Mo.

E_γ (keV)[a]	$J_i \rightarrow J_f$	I_γ[b]	R[c]
241.1	$(15^+) \rightarrow (14^+)$	14.7 (3.0)	1.6 (0.2)
250.6	$(11^-) \rightarrow$	4.0 (2.0)	
294.4	$(12^+) \rightarrow 10^+$	25.7	2.1 (0.2)
307.8	$\rightarrow (12^+)$	4.0 (3.0)	
367.4	$\rightarrow 10^+$	6.0 (2.0)	
443.3	$(16^+) \rightarrow (15^+)$	5.0 (1.0)	1.5 (0.3)
485.4	$(11^-) \rightarrow$	6.0 (3.0)	
487.0	$(14^+) \rightarrow (13^+)$	8.0 (2.0)	1.6 (0.2)
531.4	$8^+ \rightarrow 6^+$	35.0	1.9 (0.1)
555.3	$(16^-) \rightarrow (15^-)$	1.0 (0.3)	
565.4	$(15^-) \rightarrow (14^-)$	1.0 (0.3)	
623.9	$(15^-) \rightarrow (14^-)$	24.1	1.5 (0.2)
653.1	$(11^-) \rightarrow (9^-)$	20.4	1.9 (0.2)
663.1	$(14^-) \rightarrow (13^-)$	27.6	1.5 (0.2)
702.7	$4^+ \rightarrow 2^+$	90.1	2.0 (0.3)
714.7	$(15^+) \rightarrow (14^+)$	3.0 (1.5)	
728.7	$(9^-) \rightarrow (7^-)$	23.7	1.9 (0.3)
757.5	$(7^-) \rightarrow 5^-$	13.5	2.2 (0.3)
791.2	$(17^+) \rightarrow (16^+)$	3.0 (0.6)	
850.3	$6^+ \rightarrow 4^+$	72.0	1.9 (0.2)
871.6	$2^+ \rightarrow 0^+$	100.0	2.0 (0.2)
942.3	$10^+ \rightarrow 8^+$	32.4	1.9 (0.3)
944.7	$(7^-) \rightarrow 6^+$	6.7 (0.4)	1.3 (0.2)
974.4	$(14^+) \rightarrow (13^+)$	2.0 (0.5)	
984.3	$(13^-) \rightarrow (11^-)$	27.5	1.9 (0.3)
1037.5	$5^- \rightarrow 4^+$	13.0	1.3 (0.2)
1060.0	$(15^+) \rightarrow (14^+)$	3.0 (0.7)	1.6 (0.3)
1062.5	$(17^-) \rightarrow (16^-)$	11.0	1.5 (0.2)
1245.0	$(18^+) \rightarrow (17^+)$	$\leqslant$ 1.0	
1341.4	$(16^+) \rightarrow (15^+)$	6.0 (1.5)	1.5 (0.3)
1367.1	$(16^+) \rightarrow (15^+)$	9.2 (2.0)	1.6 (0.3)
1431.3	$\rightarrow (15^-)$	$\leqslant$1.0	
1542.7	$(13^-) \rightarrow (12^+)$	2.0 (1.0)	
1599.7	[d]	1.0	
1609.1	$(18^+) \rightarrow (17^+)$	3.0 (1.0)	
1612.3	$(13^+) \rightarrow (12^+)$	13.5	1.6 (0.2)
1740.1	$(17^+) \rightarrow (16^+)$	3.0 (1.0)	
1750.3	$(14^+) \rightarrow (13^+)$	8.7 (2.0)	1.6 (0.3)
2095.6	$(14^+) \rightarrow (13^+)$	4.0 (1.0)	
2188.6	$(13^+) \rightarrow (12^+)$	4.0 (1.0)	
2389.0	$(13)^+ \rightarrow (12)^+$	4.0 (1.0)	

[a]The transitions of energies $\leqslant$1500 keV are known to $\sim$0.4 keV; for the higher energies the uncertainties are $\sim$1 keV.

[b]Except where stated, the uncertainties in relative intensities are less than 10%.

[c]A blank space is kept for all the transitions for which no ratio R could be obtained.

[d]The 1600-keV transition feeds the 1431-keV transition.

adding by their presence confidence in the proposed level scheme.

Two major changes are found in the present work with respect to Ref. [4]: (i) the 449- and 84-keV transitions, placed in parallel with the 531-keV transition, have not been observed in the present work, and (ii) the 367- and 485-keV transitions have been placed above the 531-keV transition (8^+ level) and in parallel to the 942-keV transition. This change in placement is based on the coincidence relationships which show that these transitions are feeding the 10^+ level.

The level structure of ^{95}Mo was known up to $J = 23/2^+$ and an excitation energy of about 3.6 MeV from earlier work using the ^{92}Zr$(\alpha,n)^{95}$Mo and ^{94}Zr$(\alpha,3n)^{95}$Mo reactions [4]. In all, 27 new γ transitions were observed in this nucleus and the level scheme, presented in Fig. 3, has been extended up

TABLE II. Energies, initial and final spins, relative intensities, and ratio R (as defined in the text) for transitions assigned to ^{95}Mo.

E_γ (keV)[a]	$J_i \rightarrow J_f$	I_γ[b]	R[c]
153.1	$19/2^+ \rightarrow 17/2^+$	50.2	1.6 (0.2)
347.8	$17/2^+ \rightarrow 15/2^+$	50.2	1.5 (0.2)
385.2	$(11/2^-) \rightarrow 9/2^+$	5.0 (1.0)	1.3 (0.3)
387.3	$(27/2^+) \rightarrow (25/2^+)$	10.5 (1.0)	2.2 (0.3)
421.1	$9/2^+ \rightarrow 7/2^+$	2.0 (0.5)	
467.3	$7/2^+ \rightarrow 5/2^+$	2.0 (0.5)	
468.9	$(29/2^+) \rightarrow (25/2^+)$	7.0	2.2 (0.3)
535.3	$(39/2^+) \rightarrow (37/2^+)$	7.1	1.6 (0.3)
535.4	$(27/2^+) \rightarrow (25/2^+)$	21.0	1.5 (0.2)
593.2	$11/2^+ \rightarrow 9/2^+$	51.1	1.6 (0.2)
604.4	$(9/2^+) \rightarrow 9/2^+$	13.5	1.7 (0.4)
642.5	$(29/2^+) \rightarrow (27/2^+)$	33.2	1.5 (0.3)
667.4	$(13/2^+) \rightarrow (9/2^+)$	13.5	2.1 (0.3)
676.3	$(17/2^+) \rightarrow (13/2^+)$	13.5	1.9 (0.3)
691.7	$15/2^+ \rightarrow 11/2^+$	70.1	2.1 (0.3)
742.6	$(41/2^+) \rightarrow (39/2^+)$	7.1 (0.7)	1.5 (0.2)
760.0	$(15/2^-) \rightarrow (11/2^-)$	5.0 (1.0)	2.1 (0.3)
766.1	$7/2^+ \rightarrow 5/2^+$	20.0	1.5 (0.3)
770.3	$(21/2^+) \rightarrow (19/2^+)$	13.5	1.6 (0.3)
774.4	$11/2^+ \rightarrow 7/2^+$	20.0	1.9 (0.3)
855.3	$(33/2^+) \rightarrow (29/2^+)$	25.4	1.8 (0.3)
904.8	$(23/2^+) \rightarrow 19/2^+$	40.1	1.8 (0.3)
947.3	$9/2^+ \rightarrow 5/2^+$	98.0	2.0 (0.2)
950.1	$(25/2^+) \rightarrow (23/2^+)$	43.3	1.6 (0.3)
966.1	$(31/2^+) \rightarrow (29/2^+)$	10.0	1.6 (0.3)
1037.2	$(19/2^-) \rightarrow (15/2^-)$	5.0 (1.0)	1.9 (0.3)
1070.4	$(25/2^+) \rightarrow (21/2^+)$	13.5	2.2 (0.3)
1221.3	$(31/2^+) \rightarrow (31/2^+)$	4.0 (0.9)	
1266.0	$(23/2^-) \rightarrow (19/2^-)$	4.0 (1.0)	2.2 (0.3)
1277.8	$(41/2^+) \rightarrow (37/2^+)$	14.2	1.9 (0.2)
1444.7	$(45/2^+) \rightarrow (41/2^+)$	18.1	1.9 (0.3)
1500.0	$(27/2^-) \rightarrow (23/2^-)$	4.0 (1.0)	2.3 (0.4)
1531.0	$(31/2^-) \rightarrow (27/2^-)$	3.0 (1.0)	
1670.9	$(37/2^+) \rightarrow (33/2^+)$	21.2	
1861.4	$(49/2^+) \rightarrow (47/2^+)$	8.3 (2.0)	
1873.0	$(35/2^-) \rightarrow (31/2^-)$	2.0 (0.5)	
2093.2	$(31/2^+) \rightarrow (29/2^+)$	3.0 (0.5)	1.4 (0.3)
2103.4	$(35/2^+) \rightarrow (33/2^+)$	3.0 (0.5)	1.6 (0.2)

[a]The transitions of energies $\leqslant$1500 keV are known to $\sim$0.4 keV; for the higher energies the uncertainties are $\sim$1 keV.

[b]Except where stated, the uncertainties in relative intensities are less than 10%.

[c]A blank space is kept for all the transitions for which no ratio R could be obtained.

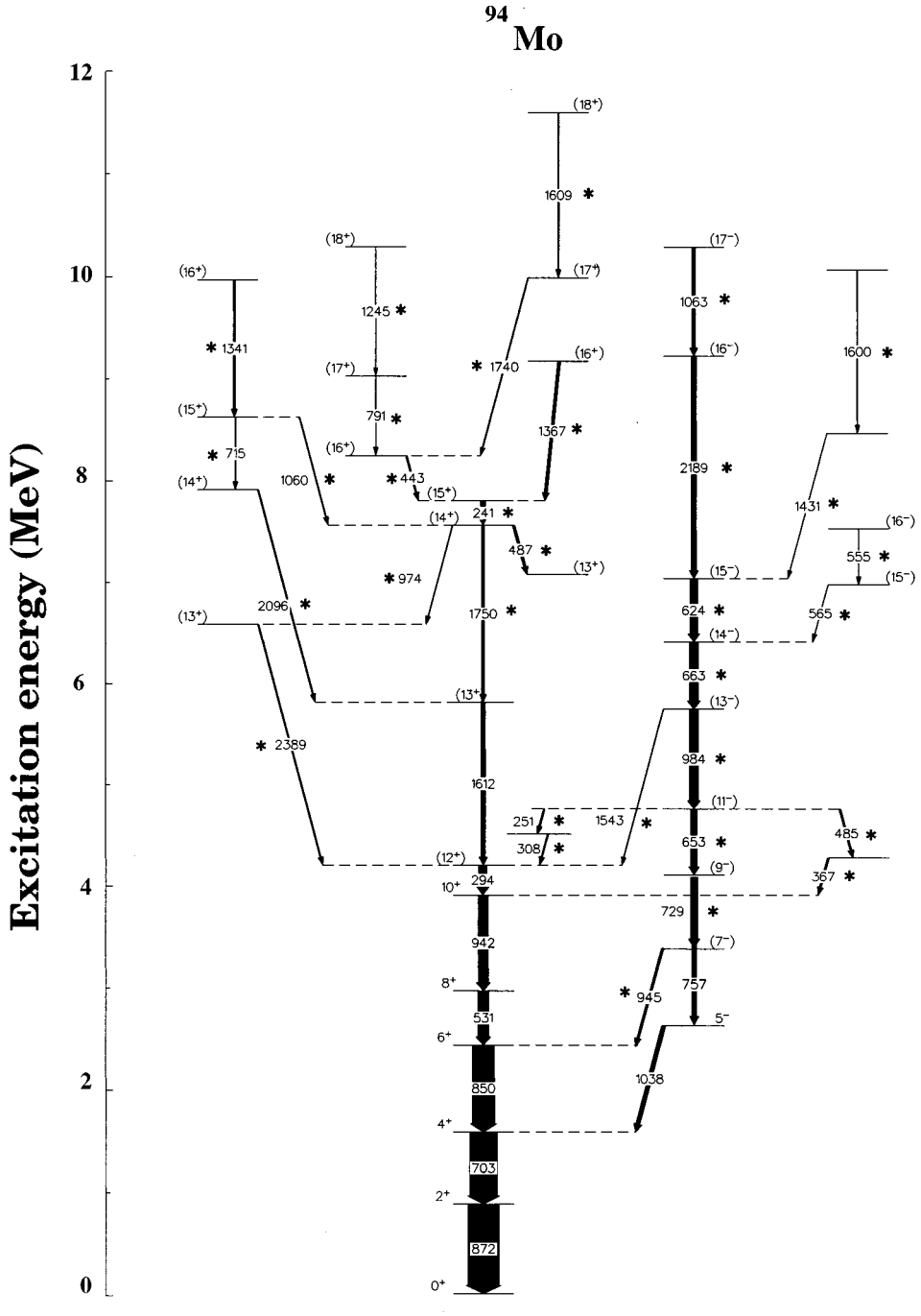

FIG. 2. Level scheme of ^{94}Mo as established from the present study. The energies are labeled in keV. The new transitions are indicated by asterisks. The widths of the arrows are approximately equal to the relative intensities of the observed γ transitions.

to $J^{\pi}=[(49/2^{+})$ and $(35/2^{-})]$. Above the ground-state transition (947 keV), the positive-parity cascade splits into two parallel sequences. Most of the intensity feeds through the level sequence starting with the 593-keV ($M1$) transition (''sequence 1''; a representative coincidence spectrum is shown in Fig. 4). The second sequence (''sequence 2'') is comprised of three previously known 604-, 387-, and 676-keV lines, to which three new 667-, 770-, and 1070-keV transitions have now been added. Figure 5 shows a representative double-gated coincidence spectrum for this sequence, and the relevant spectroscopic data for all γ rays assigned to ^{95}Mo can be found in Table II. The most important change in the level scheme with respect to Ref. [4] is that a positive parity is suggested for sequence 2 while the authors of Ref. [4] had suggested a negative parity beyond the $(9/2^{+})$ level. The ambiguity with the parity assignment for this sequence in Ref. [4] can be attributed to the fact that in that work the 387–385-keV doublet could not be separated and this precluded a firm multipolarity assignment for the 387-keV transition. The DCO ratio of the 385-keV transition is $R=1.3$—this is a typical value for an $E1$ transition—while all the γ rays at higher spin appear to be of $E2$ character. Therefore, a negative parity has been proposed for this $E2$ cascade. This cascade is very weakly populated, with the relative intensities of several transitions equal within the error limits. The actual ordering of the transitions could, there-

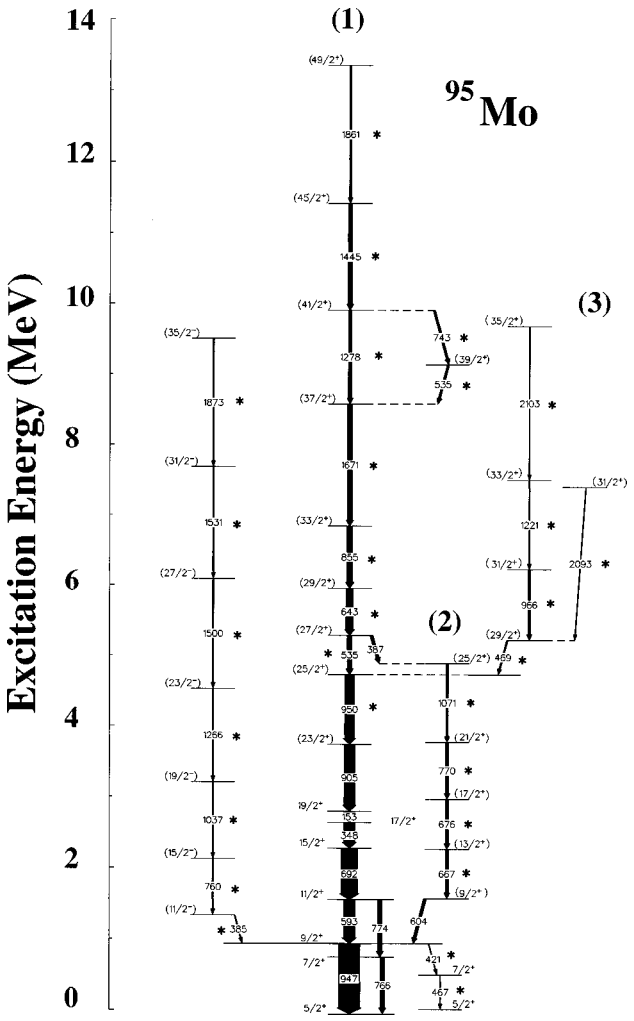

FIG. 3. Level scheme of ^{95}Mo as established from the present study. The energies are labeled in keV. The new transitions are indicated by asterisks. The widths of the arrows are approximately equal to the relative intensities of the observed γ transitions.

fore, be somewhat different from that proposed here. Consequently, although the energies of these $E2$ transitions appear to increase monotonically with spin, it would be premature to interpret this sequence as a rotational cascade.

A few other differences with respect to the work of Ref. [4] should be pointed out. These are that (i) the 174- and 1111-keV transitions, placed in parallel with the 692- and 593-keV transitions (connecting the $[(15/2^+)$ and $9/2^+]$ levels) have not been observed in the present work; (ii) the 786-keV ($M1$) transition feeding the $7/2^+$ level is also absent; and (iii) the intensities of the 766- and 774-keV transitions are $\sim$20% of that of the 947-keV line, while $\sim$50% and 38%, respectively, were reported for these two γ rays in Ref. [4]. In another study, of the low-lying states of ^{95}Mo populated in the decays of ^{95m}Tc and ^{95}Tc [17,18], a 467-keV transition has been reported as decaying from the $11/2^+$ level. This transition has not been observed in this work. However, the data show two new transitions (467 and 421 keV) parallel to the 948-keV ground-state transition.

Sequences ''1'' and ''2'' meet at the $(27/2^+)$ level. The energies of the new members of the main positive-parity cascade are of energies 950, 535 (a doublet), 643, 855, 1671, 1278, 1445, and 1861 keV. These transitions have been placed above the 905-keV $[(23/2^+)\rightarrow(19/2^+)]$ transition. Another fragmentation of γ decay in ''sequence 1'' occurs at $J=(25/2^+)$. The new cascade (called ''sequence 3'') consists of the 469($E2$)-, 966($M1$)-, 1221($M1$)-, 2093($M1$)-, and 2103($M1$)-keV transitions. The $\sim$2-MeV transitions appear in parallel with each other and are likely indicative of the breaking of the $N=50$ core. A similar feature has been reported for the $^{96-98}$Ru nuclei [10], and was interpreted as suggestive of a change in the structure following the breaking of the $N=50$ core.

IV. DISCUSSION

Several theoretical investigations have been devoted to the study of nuclei in the $N\geqslant 50$ region in order to explain the observed level structures in terms of different models, such as the shell model [2,19] or the vibrational-core model [6]. The success of the shell model in explaining the low-spin level structure of ^{95}Tc ($N=52$) [19], ^{96}Ru ($N=52$) [10] and the low-lying levels ($J\leqslant 10\hbar$) in ^{94}Mo [3] makes it imperative to attempt an understanding of the ^{94}Mo ($N=52$) high-spin level structure within the same framework. Spherical shell-model calculations using the code OXBASH [20] have been carried out for ^{94}Mo with ^{88}Sr as the inert core and the $[\pi(p_{1/2},g_{9/2});\nu(d_{5/2},s_{1/2})]$ valence orbitals. The effective interaction was taken from the work of Gloeckner [21]. Within this limited configuration space, the maximum angular momentum possible for ^{94}Mo (with four valence protons and two valence neutrons) is $J=16\hbar$. Figure 6 shows a comparison of the experimental excitation energies with the shell-model predictions denoted as GL. It is evident from the figure that the experimental results are in very good agreement with the calculations up to 12^+ and 13^-. However, a discrepancy is observed for higher levels, suggesting that this restricted model space is no longer appropriate in describing the higher spins. For example, the calculations lead to a much larger gap between the levels 12^+ and 13^+ than observed. This discrepancy may be attributed, at least in part, to contributions from configurations which were not incorporated in this restricted model-space.

The decay scheme of ^{94}Mo exhibits noticeable changes at and above the level $J=12\hbar$, with the following characteristics: (i) γ rays with energies much higher ($E_\gamma\geqslant 1.5$ MeV) than observed for lower-spin states are present, and (ii) some of these high-energy transitions appear in parallel with each other at spins where the experiment and GL model are in disagreement. These observations hint at the breaking of the $N=50$ core, suggesting that the states above $J=12\hbar$ could be dominated by the excitation of $g_{9/2}$ neutrons into higher orbitals, such as $\nu(g_{7/2},h_{11/2})$. Very recently, similar features have been observed in the $^{96-98}$Ru isotopes and were attributed to the breaking of the $N=50$ core [10].

An adequate description for the higher-angular-momentum states ($J\geqslant 12\hbar$) may, then, be sought in shell-model calculations performed with a model space encompassing all the aforementioned configurations. Such calculations, with the model space comprised of the orbitals $[\pi(f_{5/2},p_{3/2},p_{1/2},g_{9/2},g_{7/2},d_{5/2},d_{3/2},s_{1/2})$ and $\nu(f_{5/2},p_{3/2},p_{1/2},g_{9/2},d_{5/2},d_{3/2},s_{1/2},h_{11/2})]$ have been carried out: this particular model space is code named SNE in OXBASH [20]. The two-body matrix elements employed in SNE were gener-

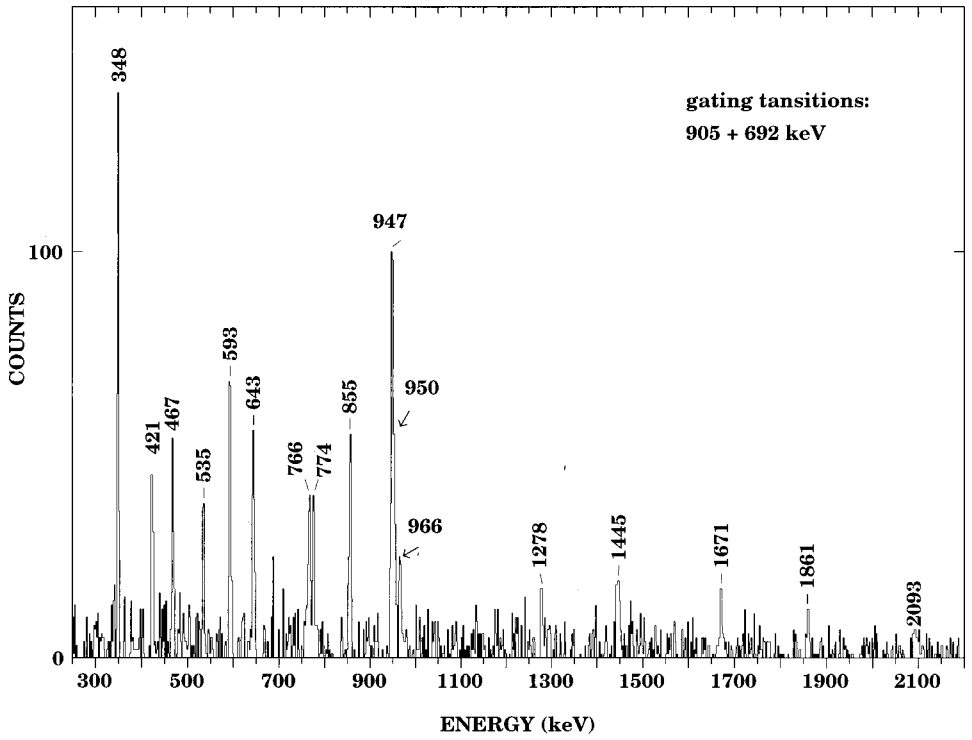

FIG. 4. Representative double-gated coincidence γ spectrum for the main positive-parity sequence of ^{95}Mo. All transition energies are marked to within ± 1 keV.

ated from a schematic interaction, with experimental values used wherever available [21], and the truncation procedure described in Ref. [22] was used. Initially, no neutron excitation across the $N=50$ core was allowed for levels below $J=16\hbar$, and the $\pi(f_{5/2},p_{3/2})$ orbitals were kept fully occupied (i.e., no excitations from these orbitals were allowed within the fpg subspace). As seen from Fig. 6, although the gap between levels 12^+ and 13^+ has been reduced, there is good agreement between the observed excitation energies and the shell-model predictions (using SNE) only for states up to $J \leqslant 13^+$ and 14^- corresponding to an improvement of only 1 spin unit compared to the GL code. Significant discrepancies still exist for higher levels. For example, the SNE-calculated 14^+, 15^+, and 16^+ levels lie at much lower ex-

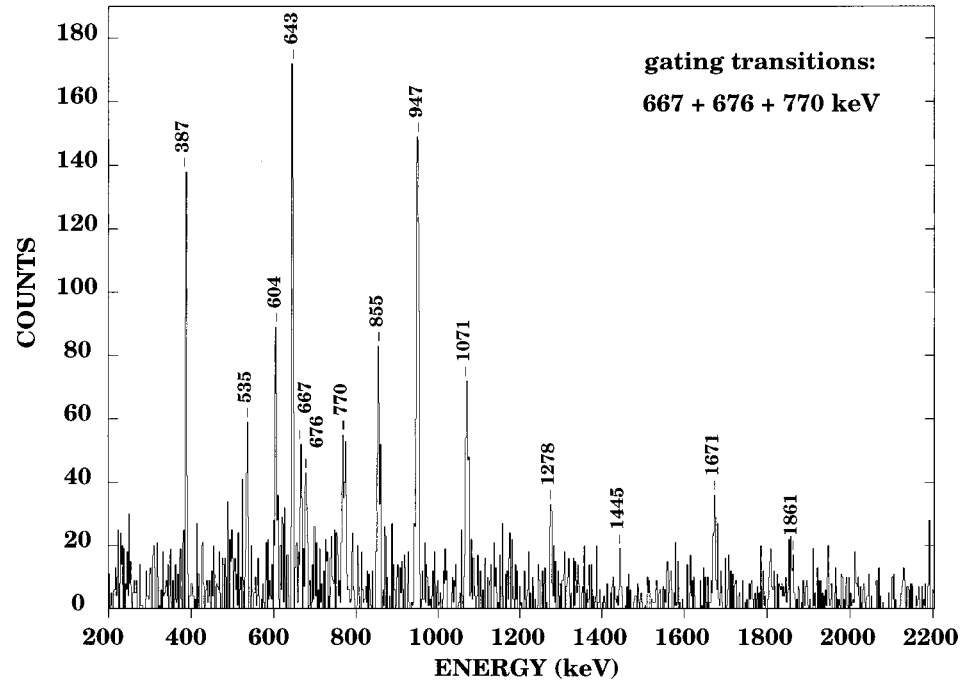

FIG. 5. Representative double-gated coincidence γ spectrum for ''sequence 2'' in ^{95}Mo. All transition energies are marked to within ± 1 keV.

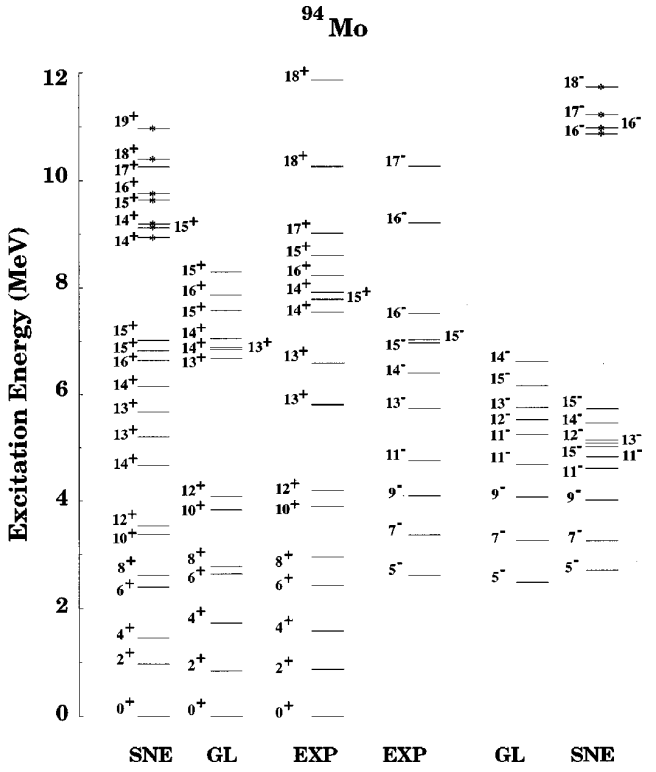

FIG. 6. Comparison of the experimental and calculated excitation energies in ^{94}Mo with shell-model predictions. See the text for the details on the various model spaces used (GL, SNE, and NU). The levels marked with an asterisk in the calculations identified by the code NU include a $g_{9/2}$ neutron excitation across the shell gap.

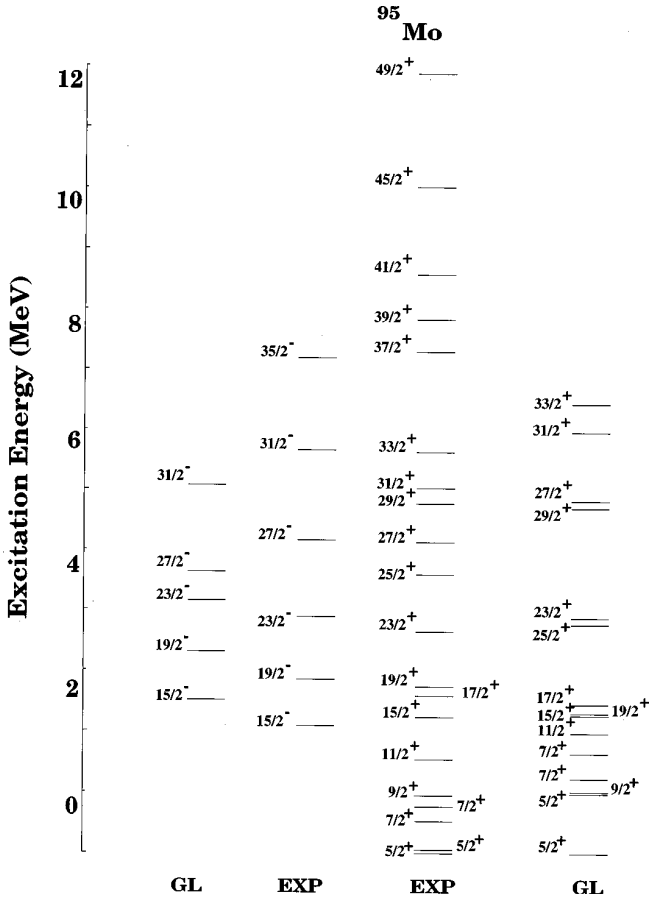

FIG. 7. Comparison of the experimental level scheme and the shell-model calculations within the GL model space for ^{95}Mo.

citation energies than the lowest experimental states with these spins. It could be surmised, then, that these states have a dominant contribution from the excitation of a $g_{9/2}$ neutron across the $N=50$ magic core. To test this hypothesis, calculations have been performed for the higher-angular-momentum states ($J \geqslant 14^+, 16^-$) by incorporating the excitation of a single $g_{9/2}$ neutron across the $N=50$ core into the next major oscillator shell [i.e., to the $\nu(d_{5/2}, g_{7/2}, s_{1/2})$ orbitals]. The configuration involving the excitation of a $g_{9/2}$ neutron into the $h_{11/2}$ orbital could not be included in the calculations due to the large dimensionality of the matrices. The results of these calculations are also presented in Fig. 6 (marked NU). Very large gaps occur in the calculations above the 13^+ and 15^- levels and, clearly, discrepancies still remain between theoretical and experimental excitation energies for the high-spin levels. A similar feature has been observed in the ^{96}Ru [10] nucleus. As in that work, the discrepancies seen here can be attributed to either (i) the effective interactions used or (ii) the truncation of the active model space. The effective interactions are not well known for such large model spaces, especially for the configurations involving the excitation of the $g_{9/2}$ neutron across the $N=50$ core, and it is our hope that the present data will lead to the development of effective interactions more suited to the high-spin states in this mass region. The effects of truncation, on the other hand, could, perhaps, be minimized by normalizing the excitation energies of the levels predicted by the shell model with the experimental value for one of the high-lying states (say, $J=14^+, 16^-$). Such normalizations have been adopted in the past by Kabadiyski *et al.* [23] to explain the high-spin states in ^{90}Mo.

The shell-model calculations described above, nonetheless, provide a qualitative understanding of the observed ^{94}Mo level structure: states with $J \leqslant 13^+, 15^-$ are dominated by neutron excitations within the $\nu(d_{5/2}, s_{1/2}, g_{7/2}, h_{11/2})$ orbitals coupled to proton excitations within the $\pi(p_{1/2}, g_{9/2})$ orbitals; the higher-spin levels are dominated by excitations involving the breaking of the $N=50$ core and the excitation of at least one $g_{9/2}$ neutron across the gap.

The $N=53$ nucleus ^{95}Mo lies in the crucial transitional region where one generally expects a transition from a spherical to a deformed shape. In attempting to understand the underlying structure of the observed levels, shell-model calculations have been performed for this nucleus using the model space GL described above. The results of these calculations are compared with the experimental levels in Fig. 7. In this case too, the agreement between theory and experiment is reasonable up to moderate spins ($J \approx 23/2\hbar$). The discrepancies for the $J=7/2^+$, $11/2^+$, and $19/2^+$ states can be attributed to the omission of the $g_{7/2}$ neutron orbital in this limited configuration space. Also, in analogy with the situation in ^{94}Mo, the higher-angular-momentum states ($J \geqslant 23/2\hbar$) are most likely dominated by the excitations of neutrons into the $g_{7/2}, h_{11/2}$ orbits which were not included in the GL model space. It would clearly be of interest to extend

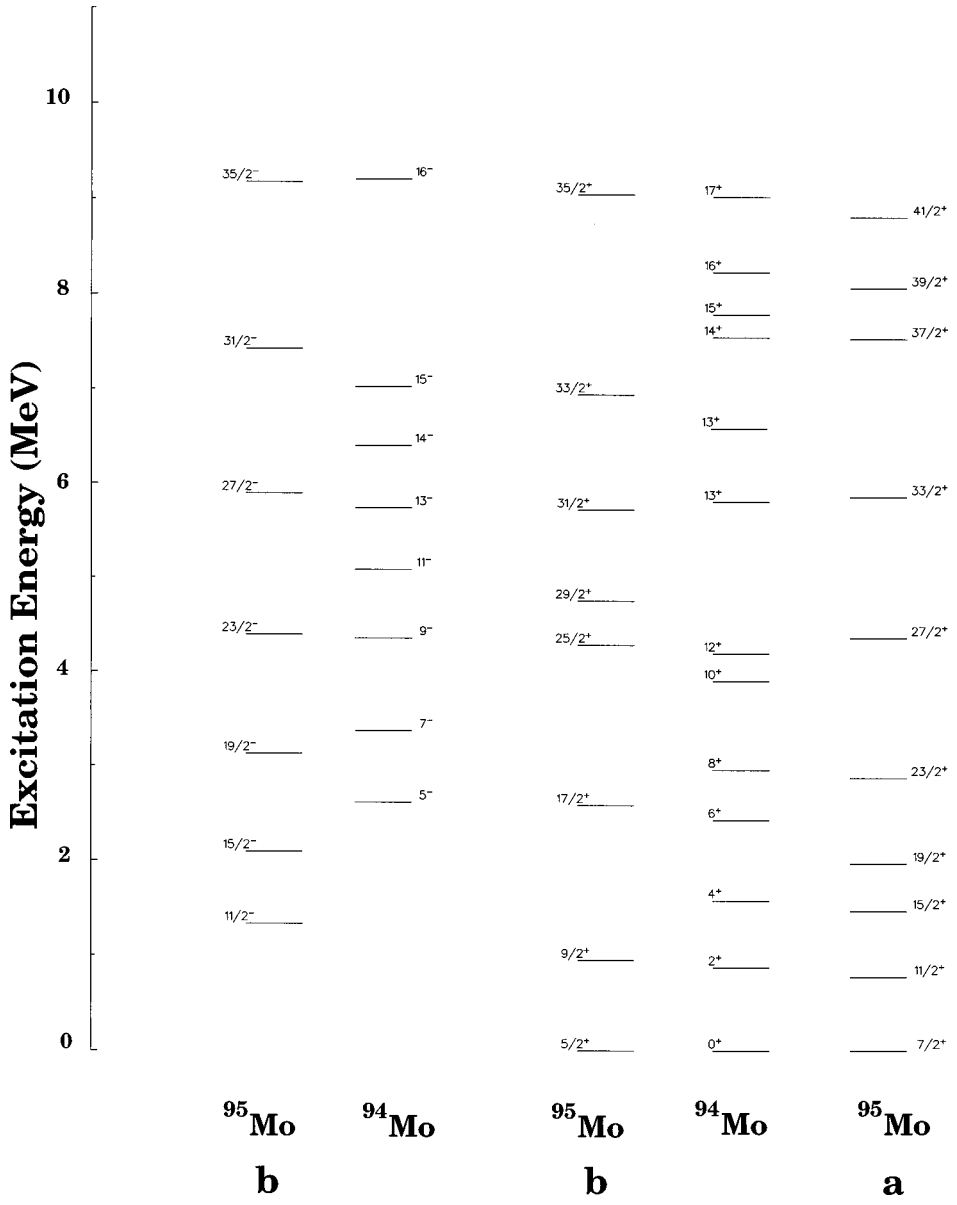

FIG. 8. Comparison of the experimentally observed level sequences of ^{94,95}Mo within the weak-coupling framework: (a) $^{94}\mathrm{Mo}(J)\otimes\nu(g_{7/2})=^{95}\mathrm{Mo}(J')$; (b) $^{94}\mathrm{Mo}(J)\otimes\nu(d_{5/2})=^{95}\mathrm{Mo}(J')$.

the calculations to a larger model space. Unfortunately, such large-basis calculations could not be undertaken due to computational limitations. In the isotone ^{97}Ru, similar conclusions have been drawn from the comparison of the data with the shell-model calculations [10]. However, it was found that the weak-coupling scheme could also provide a qualitative description of the level sequences in ^{97}Ru [10]. Therefore, similar calculations have been performed for the level sequences in ^{95}Mo. This nucleus is then described as resulting from the coupling of either a $d_{5/2}$ or a $g_{7/2}$ neutron to the ^{94}Mo core. Figure 8 illustrates the results of this stretched weak-coupling scheme for ^{95}Mo. The levels dominated by the coupling of a $\nu g_{7/2}$ neutron to the ^{94}Mo core lie about 800 keV higher in excitation energy when compared to the corresponding levels in ^{94}Mo since the $g_{7/2}$ orbital has an excitation energy of about 800 keV with respect to the $d_{5/2}$ orbital, as deduced from the excitation energy of the $7/2^+$ level in ^{95}Mo. The low-lying level structure in ^{95}Mo (up to a spin of $J\leqslant 27/2\hbar$) is clearly well reproduced by the weak-coupling scheme. Further, the stretched configuration $[^{94}\mathrm{Mo}(J)\otimes\nu(g_{7/2})=^{95}\mathrm{Mo}(J')]$ succeeds in reproducing the excitation energies of the $J=7/2^+$ and $11/2^+$ levels, which are not reproduced well in the shell-model calculations described above. This too supports the view that these states are dominated by excitations of neutrons into higher orbits like $g_{7/2}$. However, the weak-coupling approach does not appear to work very well for negative-parity states with $J\geqslant 27/2^-$. A possible explanation for this observation might be that the dominant contributions to the higher-lying states come from configurations involving other orbitals, like $\nu(h_{11/2},d_{3/2})$.

As mentioned earlier, the level scheme of ^{95}Mo contains a sequence of transitions [between the levels $J=(35/2^-)$ and $J=(11/2^-)$] with energies that appear to increase monotonically (and in a very regular manner) with spin. All these transitions are found to be of quadrupole nature from the

DCO ratio analysis and can be assumed to be $E2$'s. It is tempting to think of this sequence, therefore, as a ''rotational'' band based on the $h_{11/2}$ neutron orbital. However, our results, while intriguing, are far from definitive and point to the need for further investigation, including lifetime measurements, before a fuller understanding of the underlying nuclear structure can be achieved. Such caution is further warranted since it transpires that both shell-model and weak-coupling calculations can reproduce the lower three levels of the $E2$ sequence in ^{95}Mo quite well. Indeed, it has been pointed out previously by Skouras and Dedes [19] that the excitation energies of nuclei in this transitional region can be reproduced more or less equally well by both the spherical shell model and the collective (particle + vibrating core) model, rendering a clear distinction between the two modes quite difficult in the absence of additional spectroscopic data.

V. SUMMARY

The ^{36}S+^{65}Cu reaction at an incident beam energy of 142 MeV has been used to populate the high-spin states in ^{94,95}Mo ($N=52,53$) and γ-ray spectroscopic measurements have been performed with the Early Implementation Gammasphere detector array. In ^{94}Mo, the observed level sequences (up to a tentative spin of $J=18\hbar$ and an excitation energy of $E_x\approx 12$ MeV) can be interpreted in terms of the spherical shell model. The low-lying levels (up to $J\sim 13\hbar$) can be described quite satisfactorily by single-particle excitations involving the $[\pi(p_{1/2},g_{9/2});\ \nu(d_{5/2},s_{1/2},g_{7/2},h_{11/2})]$ orbitals. The higher-angular-momentum states are, most likely, dominated by the excitation of a single neutron across the $N=50$ closed shell into the next major oscillator shell. The level scheme of ^{95}Mo has been extended to ($J=49/2^+$, $35/2^-$, $E_x\approx 12$ MeV). The level structure can be described rather satisfactorily in the framework of the stretched coupling scheme, with a $d_{5/2}$ or $g_{7/2}$ neutron weakly coupled to the ^{94}Mo core, as well as by shell-model calculations using a limited configuration space (GL).

ACKNOWLEDGMENTS

The authors acknowledge the help received from B. Prause, Dr. G. Smith, and the Gammasphere support staff during the experiment. This work was supported in part by the U.S. National Science Foundation (Grant No. PHY94-02761), the U.S. Department of Energy (Contracts Nos. W-31-109-ENG-38 and DE-FG05-87ER40361), and the Polish-American Maria Sklodowska-Curie Joint Fund II (Project No. PAA/DOE-93-153).

[1] S. S. Ghugre, S. Naguleswaran, R. K. Bhowmik, U. Garg, S. B. Patel, W. Reviol, and J. C. Walpe, Phys. Rev. C **51**, 2809 (1995).
[2] S. S. Ghugre, S. B. Patel, M. Gupta, R. K. Bhowmik, and J. A. Sheikh, Phys. Rev. C **47**, 87 (1993).
[3] C. M. Lederer, J. M. Jaklevic, and J. M. Hollander, Nucl. Phys. **A169**, 449 (1971).
[4] C. M. Lederer, J. M. Jaklevic, and J. M. Hollander, Nucl. Phys. **A169**, 489 (1971).
[5] L. Mesko, A. Nilsson, S. A. Hjorth, M. Brenner, and O. Holmlund, Nucl. Phys. **A181**, 566 (1972).
[6] D. G. Sarantites, Phys. Rev. C **10**, 2348 (1974).
[7] J. B. Ball, J. B. McGrory, R. L. Auble, and K. H. Bhatt, Phys. Lett. **29B**, 182 (1969).
[8] H. A. Roth, S. E. Arnell, D. Foltescu, O. Skeppstedt, J. Blomqvist, A. Nilsson, T. Kuroyanagi, S. Mitarai, and J. Nyberg, Phys. Rev. C **50**, 1330 (1994).
[9] P. Singh, R. G. Pillay, J. A. Sheikh, and H. G. Devare, Phys. Rev. C **45**, 2161 (1992).
[10] B. Kharraja, S. S. Ghugre, U. Garg, M. P. Carpenter, B. Crowell, R. V. F. Janssens, T. L. Khoo, T. Lauritsen, D. Nisius, W. Mueller, W. Reviol, L. L. Riedinger, and R. Kaczarowski, Phys. Rev. C **57**, 83 (1998).
[11] D. C. Radford, I. Ahmad, R. Holzmann, R. V. F. Janssens, and T. L. Khoo, Nucl. Instrum. Methods Phys. Res. A **258**, 111 (1987).
[12] J. A. Kuehner, J. C. Waddington, and D. Prevost, in ''Proceedings of the International Conference on Nuclear Structure at High Angular Momentum,'' Ottawa, 1992, edited by J. C. Waddington and D. Ward, Report No. AECL-10613, 1992, p. 413.
[13] D. C. Radford, Nucl. Instrum. Methods Phys. Res. A **361**, 297 (1995).
[14] G. Palameta and J. C. Waddington, Nucl. Instrum. Methods Phys. Res. A **234**, 476 (1985).
[15] B. Crowell, M. P. Carpenter, R. G. Henry, R. V. F. Janssens, T. L. Khoo, T. Lauritsen, and D. Nisius, Nucl. Instrum. Methods Phys. Res. A **355**, 575 (1995).
[16] J. Gizon, D. Jerrestam, A. Gizon, M. Jozsa, R. Bark, B. Fogelberg, E. Ideguichi, W. Klamra, T. Lindblad, S. Mitarai, J. Nyberg, M. Piiparinen, and G. Sletten, Z. Phys. A **345**, 335 (1993).
[17] G. Chilosi, E. Eichler, and N. K. Aras, Nucl. Phys. **A123**, 327 (1969).
[18] T. Cretzu, K. Hohmuth, and J. Schintlmeister, Nucl. Phys. **70**, 129 (1965).
[19] L. D. Skouras and C. Dedes, Phys. Rev. C **15**, 1873 (1977).
[20] B. A. Brown, A. Etchegoyen, W. D. M. Rae, and N. S. Godwin (unpublished).
[21] D. H. Gloeckner, Nucl. Phys. **A253**, 301 (1975).
[22] S. S. Ghugre and S. K. Datta, Phys. Rev. C **52**, 1881 (1995).
[23] M. K. Kabadiyski, F. Cristancho, C. J. Gross, A. Jungclaus, K. P. Lieb, D. Rudolph, H. Grawe, J. Heese, K.-M. Maier, J. Eberth, S. S. Koda, W. T. Chow, and E. K. Warburton, Z. Phys. A **343**, 165 (1992).